INTERNATIONAL ATOMIC ENERGY AGENCY
UNITED NATIONS EDUCATIONAL, SCIENTIFIC AND CULTURAL ORGANIZATION
INTERNATIONAL CENTRE FOR THEORETICAL PHYSICS
I.C.T.P., P.O. BOX 586, 34100 TRIESTE, ITALY. CABLE: CENTRATOM TRIESTE

SMR.380/14

COLLEGE ON THEORETICAL AND EXPERIMENTAL RADIOPROPAGATION SCIENCE

6 - 24 February 1989

LECTURES 1 & 2: GENERAL CHARACTERISTICS OF THE TROPOSHERE

G.O. AJAYI

Department of Electronic and Electrical Engineering
Obafemi Awolowo University
Ile-Ife, Nigeria

TABLE OF CONTENTS

1. INTRODUCTION

The troposphere is the lower part of the Earth's atmosphere extending to an altitude of about 9 km at the earth's poles and 17 km at the equator. The tropopause is the upper boundary of the troposphere, above which the temperature increases slightly with height or remains constant.

The percentage composition of the principal gases does not change with altitude except that of water vapour. The permanent dipole moment of the molecules of water vapour causes it to be a very significant contributor to the variability of the atmospheric refractive index. The proportion by volume of water vapour in the air at the ground level on the average varies from less than 0.001% in the arctic to more than 5% in the tropics (Hall, 1979). This proportion decreases rapidly with height and is highly dependent on local air temperature. Figures 1(a) and (b) show [Oyinloye, 1988] typical variations in Niger, West Africa and India respectively. Radiation, absorption, condensation, evaporation, advection, convection, turbulent diffusion and a number of complex and interacting meteorological phenomena lead to non-linear and fairly unpredictable processes in the troposphere. [Reddy, 1967].

The atmospheric pressure tends to decrease exponentially with altitude as

$$p = p_0 e^{-h/H} \quad \text{---} \quad (1)$$

where h is the height above a reference level where the pressure is p_0.

The scale height, H is given by

$$H = KT/mg \quad \text{---} \quad (2)$$

where T = temperature, m = average mass of the molecules present, g = acceleration due to gravity and K = Boltzmann's constant

2. THERMAL STRUCTURE

The troposphere is transparent to most of the solar energy, hence the source of the heat for the troposphere is the earth which is heated by the sun. The earth heats the troposphere through the processes of conduction, convection and radiation. The resulting thermal structure is modified by the water vapour generated from ocean surfaces and large bodies of water. The dry adiabatic lapse rate in the troposphere is 9.8 °C per km. Due to the presence of water vapour, the temperature lapse rate is less than 9.8°C per km. When an air parcel with water vapour rises up adiabatically, it expands and cooling takes place. If the water vapour density is high enough, part of this water vapour condenses and heat is added locally to the atmosphere

due to the latent heat of evaporation (Reddy, 1987). The temperature in the troposphere gradually decreases with height at the rate of approximately 6°C per km.

Temperature increases with altitude in an inversion layer and such a layer is highly stable. All vertical motions are strongly inhibited and pollution emitted below the layer tends to be confined below it. Radiation cooling causes temperature inversion. For example, on a typical warm and cloudless day, the ground cools rapidly after sunset, cooling the air in its vicinity. The air higher up remains warm with consequent positive temperature gradient. Advection can also cause temperature inversion. For example, hot dry air from land may move over cold wet air causing temperature inversion.

3. RADIO REFRACTIVE INDEX

The atmospheric radio refractive index, n is very close to unity (typically 1.00035), hence it is more convenient to talk of the refractivity, N given by

$$N = (n-1)\times 10^6 = \frac{77.6}{T}\left(p + 4810\frac{e}{T}\right) \quad \text{---} \quad (3)$$

where p = atmospheric pressure (mb)
e = water vapour pressure (mb)
T = absolute temperature (K).

Alternatively

$$N = 77.6\frac{p}{T} + 3.73\times 10^5 \frac{e}{T^2} \quad \text{----} \quad (4)$$

In eqns (4), 1st term is the dry term
2nd term is the wet term.

The relationship between water vapour density, ρ (gm/m^3), water vapour pressure, e (mb) and the relative humidity, H (%) is given by CCIR, 1986

$$\rho = 216.7 \frac{e}{T} \quad \text{---} \quad (5)$$

$$H = 100 \cdot e/e_s \quad \text{---} \quad (6)$$

$$e_s = \frac{5854}{T^5} \cdot 10^{(20-2950/T)} \quad \text{---} \quad (7)$$

where e_s = saturation vapour pressure (mb) at temperature T (K).

The dependence of refractivity on temperature and relative humidity is very important in the tropics. Figure 2 [Reddy, 1987] illustrates these changes in refractivity for varying relative humidity values at different temperatures. For example, at a relative humidity of 60%, when the temperature changes from −10°C to +10°C the variation in refractivity is negligible in contrast to much larger variation at higher temperatures, say from 20°C to 40°C. This pattern explains how surface refractivity and also the effective earth's radius factor (k) may be subjected to wild variations in a single day in the tropical region.

3.1 REFRACTIVITY IN THE MODEL ATMOSPHERE

Pressure, temperature and water vapour content all decrease with height above the earth's surface in the troposphere on the average, except in temperature inversion layers where temperature increases with height.

N varies with height as

$$N(h) = N_s \exp(-h/H) \quad \text{---} \quad (8)$$

where N(h) is refractivity at a height h above which the refractivity is N_s, H is scale height.

for the CCIR model atmosphere

$$N(h) = 315 \exp(-0.136h) \quad \text{---} \quad (9)$$

where 315 is the average surface refractivity and the scale height is 7.353 km.

h is in km.

3.2 SEA LEVEL REFRACTIVITY

For prediction of some propagation effects, the surface refractivity is useful. To remove surface height variations (topography of location) surface refractivity can be reduced to sea-level values, N_0 using

$$N_s = N_0 \exp(-0.136h) \quad \text{---} \quad (10)$$

The scale height in the locality can be used if available.

The CCIR has produced world map of N_0.

Figures 3(a) and (b) [Kolawole and Owonubi, 1982] shows the surface refractivity variation in Africa, with the following main features [Oyinloye, 1987]

(a) In the equatorial climatic belt ($\pm 5°$ latitude), N_0 is characterized by high values in the range 370 to 390 N-units and is practically independent of season. The annual range of mean N_0 is only about 5-10 N-units.

(b) In the tropical continental climatic region ($5° - 20°$ latitude), N_0 is much higher during the rainy season than during the dry season and there are high annual ranges of about 70-110 N-units.

(c) In the hot desert region ($20° - 30°$ N latitude), low values of about 310 units are found in the hinterland.

(d) In the warm temperate region, moderate values of N_0 (300-350) N-units are found with a low annual range of about 5 N-units.

Owolabi and Williams, 1970 have shown that in Nigeria, N_s decreased from the South to the North (Figure 4) and the values 375, 350 and 325 N-units were obtained for the Southern (latitude $4° - 7°$ N), middle (latitude $7° - 10°$ N) and northern (latitude $10° - 13°$ N) zones respectively. In Brazil, the values of N_0 at Belem ($1.5°$S, $48.5°$N) are about 370 and 360 N-units in

February and August respectively indicating slightly greater refractivity in local summer which coincides with the rainy season [Ponter and Akeis, 1981; Radicella, 1982]. Figure 5 shows the latitude variations of sea level refractivity in Argentina and Brazil [Oyinloye, 1987].

3.3 REFRACTIVITY GRADIENT

The curvature of the ray path in the troposphere is determined by the refractivity gradient and not by its absolute value.

From eqn (3), we have

$$\frac{dM}{dh} = 77.6\left[\frac{1}{T}\frac{dP}{dh} - \left(\frac{P}{T^2} + \frac{9620e}{T^3}\right)\frac{dT}{dh} + \frac{4810}{T^2}\frac{de}{dh}\right] m^{-1} \quad - - - (11)$$

Making use of the standard (average) gradients of pressure, temperature and water vapour at ground level for temperate latitudes in eqn (11), we have

$$\frac{dM}{dh} = -0.04\ M/m \quad - - - 12(a)$$

$$\text{or } \frac{dM}{dh} = -40\ M/km \quad - - - 12(b)$$

In eqn (11), $\frac{dP}{dh}$, $\frac{dT}{dh}$ and $\frac{de}{dh}$ are negative in a standard troposphere, thus making the second term positive and still give a small negative value of dM/dh. In a temperature inversion, when dT/dh is positive, dM/dh becomes negatively large. Since temperature inversion

large lapse rate of water vapour is produced in such layers. The combination of positive dT/dh and a large negative de/dh result in large negative values of refractivity gradient in an inversion layer.

Figure 6 [CCIR, 1986] shows an example of the world chart of ΔN, the decrease in N over the first 1km layer. ΔN is given by

$$\Delta N = N_s - N_1 \quad ---- \quad (13)$$

where N_1 = radio refractivity at a height of 1km above the surface.

Vertical gradients have also been evaluated over the lowest 100 metres for many parts of the world. Examples are [CCIR, 1986]:

(i) U.S.A. – Cape Kennedy, Florida
- 230 M/km exceeded for 0.05% of time
- 370 M/km exceeded for 99.9% of time

(ii) Japan and the U.K.
- 70 M/km exceeded for 0.1% of time
- 200 M/km exceeded for 99.9% of time

However, in the tropical region, studies indicate a percentage of extreme vertical refractivity gradients (over the first few hundred metres above ground), lying outside the range 0 to −157 M/km i.e. larger than temperate latitude values. Figure 7 shows percentage of time gradients is less or equal to −100 M/km for the month of August. [CCIR, 1988].

4. ATMOSPHERIC REFRACTION

A radio wave encounters variations in atmospheric refractive index along its trajectory that cause the ray path to become curved.

The radius of curvature, R of the ray is given by

$$\frac{1}{R} = -\frac{\cos\theta}{n}\frac{dn}{dh} \quad ---- \quad (14)$$

where θ = angle of the radio ray with the horizontal.

In the troposphere, $n \approx 1$ and for small values of angle θ, we have

$$\frac{1}{R} = -\frac{dn}{dh} = -\frac{dN}{dh} \times 10^{-6} \quad ---(15)$$

R is determined by the lapse rate of refractive index with height and not by its absolute value. When dN/dh is negative, R is positive and the propagation path is convex.

4.1 Effective Earth Radius

– A hypothetical effective earth radius that makes the relative curvature of the ray and that of an effective earth to be such that radio rays appear to travel in straight lines rather than curved lines over the true earth. This technique is adequate in a well mixed atmosphere where the refractivity gradient can be assumed to be constant with height.

By equating the relative curvatures, we have

$$a' = ka \quad - - - - - - - - - - 16(a)$$

where $k = \left(1 + a \frac{dN}{dh} \times 10^{-6}\right)^{-1}$ - - - 16(b)

and k is the effective earth radius factor. For middle latitudes, average $\frac{dN}{dh}$ for standard atmosphere is -40N-units/km and k is 4/3 There is a large variation in the median values of k near the equator. In the equatorial regions of India, k varies between 1.3 and 1.8 [Ojiuloge, 1987]. In the equatorial regions of Africa, k is 1.5 [Kolawole and Owonubi, 1982]. K was also found to be 1.43 and 1.22 for the rainy and dry seasons respectively and k of 1.20 was obtained for the desert region in Africa.

4.2 M-Profile - The M-profile technique is useful for a stratified troposphere when the refractivity gradient is no longer constant with height. The term M or "modified" refractive index has been defined in units which relate the curvature of microwave beams to the curvature of the earth.

$$M = N + 10^6 \frac{h}{a} \quad - - - 17(a)$$

$$\text{or } M = N + 157h \quad - - - 17(b)$$

Fig. 8 shows typical M-profiles [Lenkurt,

$$\frac{dM}{dh} = \frac{dN}{dh} + 157 \quad - - - (18)$$

i.e. $\frac{dM}{dh}$ is positive for $\frac{dN}{dh}$ less negative than

-157 N/km. The gradient of M is a useful indicator for occurrence of ducting.

5. FORMS OF ATMOSPHERIC REFRACTION

(a) Negative Refraction: $\frac{dN}{dh} > 0$ and R is negative

The ray paths are curved upwards. The radio wave moves away from the earth's surface and the line of sight range and the range of propagation decrease accordingly.

(b) Zero refraction: $\frac{dN}{dh} = 0$ and R is infinite

The ray is a straight line.

(c) Positive Refraction: $\frac{dN}{dh} < 0$ and R is positive

The ray paths are curved towards the earth.

Positive refraction can be subdivided into

(i) Standard: $\frac{dN}{dh} = -40$ N/km, $k = 4/3$

(ii) Critical: $\frac{dN}{dh} = -157$ N/km, $k = \infty$

(iii) Ducting: $\frac{dN}{dh} < -157$ N/km, $k < 0$

Three broad classifications of atmospheric refraction are:

Subrefraction Region	Superrefractive Region	Ducting Region
$\frac{dN}{dh} > -40$	$-157 < \frac{dN}{dh} < -40$	$\frac{dN}{dh} < -157$
$\frac{4}{3} < k < \infty$	$0 < k < 4/3$	$k < 0$
$\frac{dM}{dh} > 0$	$\frac{dM}{dh} > 0$	$\frac{dM}{dh} < 0$

figure 9 shows the actual and equivalent paths of the radio ray. fig. 10 shows variation of k with dN/dh and fig. 11 shows the bending of radio rays for constant values of dM/dh.

5.1 Super-refraction and Ducting.

Under the influence of synoptic processes such as subsidence, advection, or surface heating and radiative cooling, stratification can occur in the lower troposphere.

when $\frac{dM}{dh} < -157$ M/km we have ducting.

Ducting occurs for grazing angles of incidence θ less than or critical angle, θ_c [CCIR, 1982]

$$\theta < \theta_c = \arcsin\left(\sqrt{2|\Delta M| \times 10^{-6}}\right) \quad --(19)$$

where ΔM = change in M across a ducting layer of thickness, δ.

for efficient duct propagation, $\lambda < \lambda_c$ where

$$\lambda_c = 1.9 \times 10^{-4} D^{1.8} \quad ----(20)$$

for an elevated duct, the duct thickness D (metres) is given by (see fig. 12)

$$D = \delta \left[1 + \left|\frac{dM}{dh}\right|_\delta \Big/ \left|\frac{dM}{dh}\right|_s \right] \quad ----(21)$$

where $\left|\frac{dM}{dh}\right|_\delta = \frac{\Delta M}{\delta}$ is the magnitude of the ducting gradient

and $\left|\frac{dM}{dh}\right|_s$ = magnitude of the gradient in the underlying layer (if present)

For a ground based duct with no underlying layer, $D = 2\delta$

Tropospheric layers (e.g. near the surface) can

(i) introduce additional propagation paths, thus producing fading.

(ii) effectively isolate one communication terminal from the other.

(iii) diffract the service propagation path, introducing losses.

(iv) cause interference to other distant services

fig. 13 shows an atmospheric fading mechanism caused by isolation.

5.1.1. Surface Ducts — The occurrence of initial gradient less than -157 M/km is used as a direct measure of the occurrence of ground based ducts that are 100m thick. The sea-surface ducts tend to be more prevalent and extensive than those overland. fig. 14 shows the refractivity gradient contours for the trade wind inversion in May [Dougherty et al., 1967). fig. 15 shows the surface duct occurrence probability (%) in India for May and July at midnight [Reddy, 1982]

The radio refractivity data for Dakar in Senegal (latitude 14.7°N), Niamey in Niger (latitude 13.5°N), Fort Lamy (N'Djamena) in Chad (latitude 12.1°N), Lagos in Nigeria (latitude 6.6°N), Abidjan in Cote d'Ivoire (latitude 5.3°N) and Bangui in the Central African Republic (latitude 4.4°N) were

used by Owolabi and Ajayi, 1976 to study the surface duct occurrence probability in West Africa. The results showed that an average high surface ducting occurrence probability of 43% was found for the three stations north of latitude 12°N compared with a corresponding probability of 8% for the three stations south of latitude 12°N. In Senegal (on the Atlantic coast in Africa), Hautefeuille et al. observed very deep fading of up to 50 dB on a 7 GHz radio link.

5.1.2 Elevated Ducts: Appendix 1(a) [Dougherty and Dutton 1981] show meteorological conditions that can give rise to surface ducts. Elevated ducts also occur in practice. Appendix 1(b) shows meteorological conditions [Dougherty and Dutton, 1981] that give rise to elevated ducts.

Duct propagation can result in leakage of communication and it is also a potential source of interference to other communication services.

5.2 LOSSES IN DUCT PROPAGATION

The basic transmission loss is related to that of free space L_{bf} by [CCIR, 1982]

$$L_b = L_{bf} - 10 \log d' + A \quad ----- (22)$$

where d' = distance within the duct

L_b = duct transmission loss

The factor A accounts for other attenuation mechanisms such as leakage losses due to duct irregularities or losses due to ground reflection, etc and etc.

Note: $L_{bf} = 92.44 + 20 \log d + 20 \log f$ ---(23)

with d in km and f in GHz.

6 MEASUREMENT OF RADIO REFRACTIVITY

(a) Direct Method: Use microwave refractometer. Capable of measuring rapid fluctuations in N. The refractometer measures the change in the resonant frequency of a cylindrical cavity with ends open to the atmosphere and compare with the resonant frequency of a standard cavity sealed from the atmosphere. The refractometer is usually mounted on an aircraft for obtaining N-height profile, hence it is an expensive technique. [Refer to Figs. 16, 17 & 18].

(b) Indirect Method: N can be computed from measured pressure, temperature and water vapour pressure.

(i) Tethered balloon system can be used for height profile of less than 1 km altitude. Poor time resolution because each profile can take more than 1 hr, hence it is not a true representation of conditions at any time.

(ii) Radiosonde balloon flights at some hundreds of stations all over the world, with launches at 0000 hrs GMT and 1200 hrs GMT. Provides a large volume of data for statistical analysis. The spatial and temporal resolutions of the data are poor for radio communication applications.

(c) Sodar: This is an acoustic sounding system, which is very useful for monitoring temperature inversions which cause radio ducts.

7. REFERENCES

1. Aro, T.O. "Analysis of data on surface and tropospheric water vapour", J. Atmos. and Terr. Phys. 38, 565-571, (1976).

2. CCIR: Recommendations and Reports of the International Radio Consultative Committee, XVth Plenary Assembly - Propagation in non-ionized media, Vol. V, (1982)

3 CCIR: Recommendations and Reports of the International Radio Consultative Committee, XVIth Plenary Assembly - Propagation in non-ionized media; Vol. V, (1986).

4. CCIR: Conclusions of the Interim Meeting of Study Group 5 - Propagation in non-ionized media, Doc. 5/204-E, July 1988.

5. Dougherty, H.T. and Dutton, E.J. "The role of elevated ducting for radio service and interference fields". U.S. Dept. of Commerce, NTIA - Report -81-69, (1981).

6 Dougherty, H.T., Riggs, L.P. and Sweezy, W.B. "Characteristics of the Atlantic trade wind System significant for radio propagation", Technical Report 29, U.S. Dept. of Commerce, Institute of Telecomm. Sciences, (1967).

7. Hall, M.P.M. "Effects of the troposphere on radio Communication", Institution of Electrical Engineers, London, (1979).

8. Hamlefeuille, M., Boyle A.W., Timmers A.G.W. and Shannon J.D. "Ducting fading - is Senegal an isolated case?" Telecomm. Journal, 47, 517-525, (1980)

9 Idahosa L.B. and Owonubi J.J. "The surface radio refractivity over Africa", Nigerian Journal Science, 16, 441-454, (1982).

10 Ojo, J.O. "The Troposphere in tropical and Subtropical latitudes", in Handbook on Radio-propagation for tropical and subtropical Countries, 79-99, (1987).

11 Ojo J.O. "Characteristics of non-ionized media and radiowave propagation in equatorial areas - A review", Telecomm. Journ. 55, 115-129, (1988)

12 Owolabi, I.E. and Ajayi, G.O. "Superrefractive conditions and their implication for tropospheric radiowave propagation in West Africa", Nigerian Journ. of Science., 10, 291-313, (1976).

13 Owolabi, I.E. and Williams, V.A. "Surface radio refractivity patterns in Nigeria and the Southern Cameroons", J. West Africa Science Association, 15, 3-17, (1970).

14 Portes, M.S. and Assis, M.S. "Propagation conditions in South and Central America". Paper presented to the preparatory seminar for 1983 WARC, (1981).

15 Radicella, S.M. "Tropospheric radio propagation, Autumn course in geomagnetism, the ionosphere and magnetosphere, SMR/98-48, ICTP, Trieste, Italy, (1982).

16 Reddy, B.M. "Characterization of tropospheric environment. Autumn course on geomagnetism, the ionosphere and magnetosphere, SMR/98-44, ICTP, Trieste, Italy, (1982)

17 Reddy, B.M. "The Physics of the Troposphere, in Handbook on Radiopropagation for tropical and sub-tropical countries, (1987).

18 Segal, B. and Barrington, R.E. "The radio climatology of Canada, Tropospheric refractivity atlas for Canada, Dept. of Communications, Communications Research Centre, CRC Report No 1315-4, Ottawa, Canada, (1977)

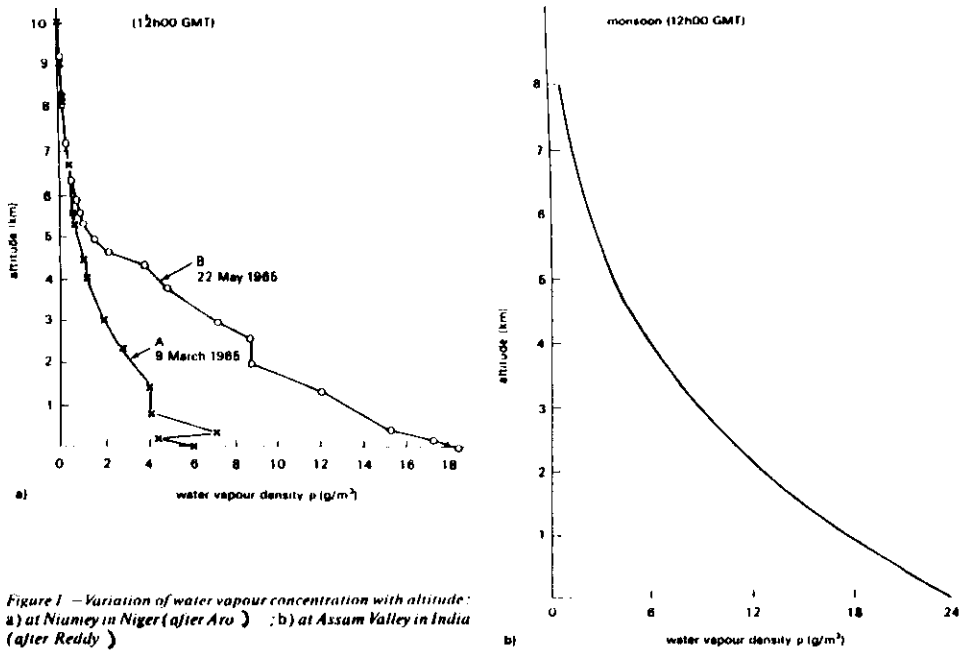

Figure 1 — Variation of water vapour concentration with altitude: a) at Niamey in Niger (after Aro) ; b) at Assam Valley in India (after Reddy)

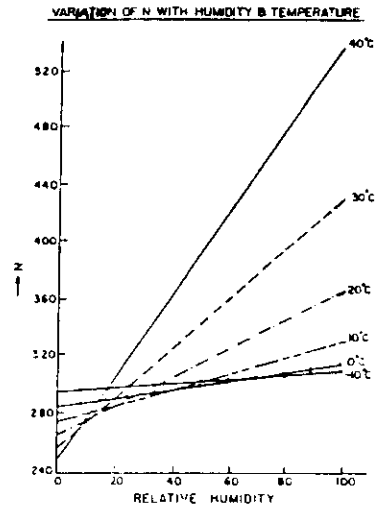

Fig. 2. Calculated values of Radio Refractivity plotted against Relative Humidity at different Temperatures. Demonstrates low dependence on Relative Humidity at low temperatures. N is sensitive at high humidities and temperatures (tropics). [After Reddy, 1987]

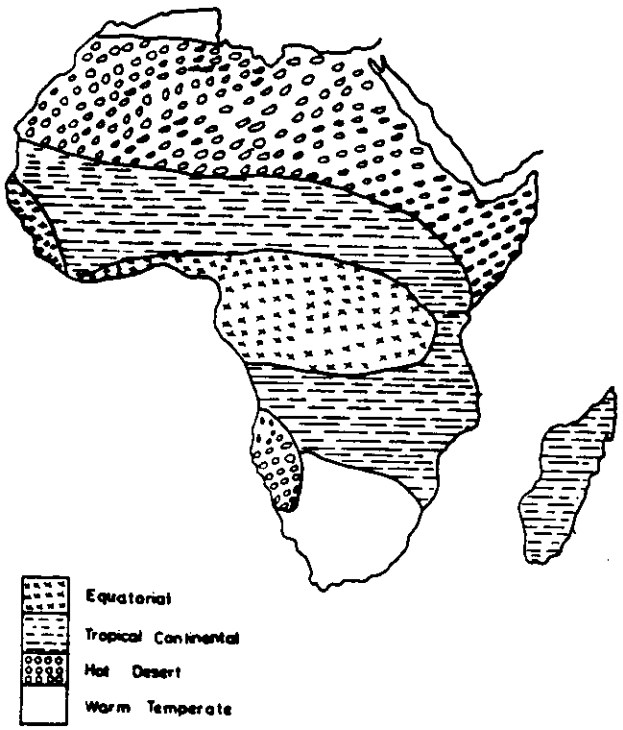

Figure 3a- Main climatic Regions of Africa.

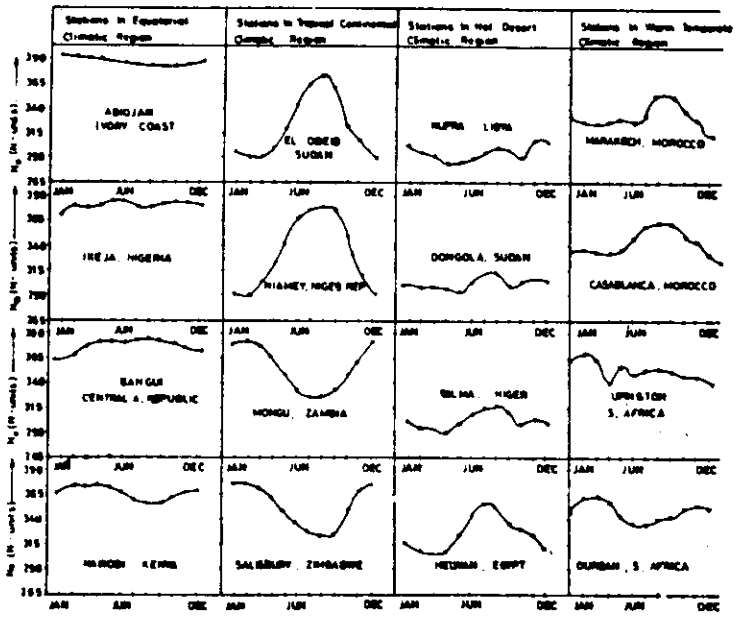

Figure 3b N_o patterns in the different climatic regions of Africa.

[After Kolawole and Awombi, 1982]

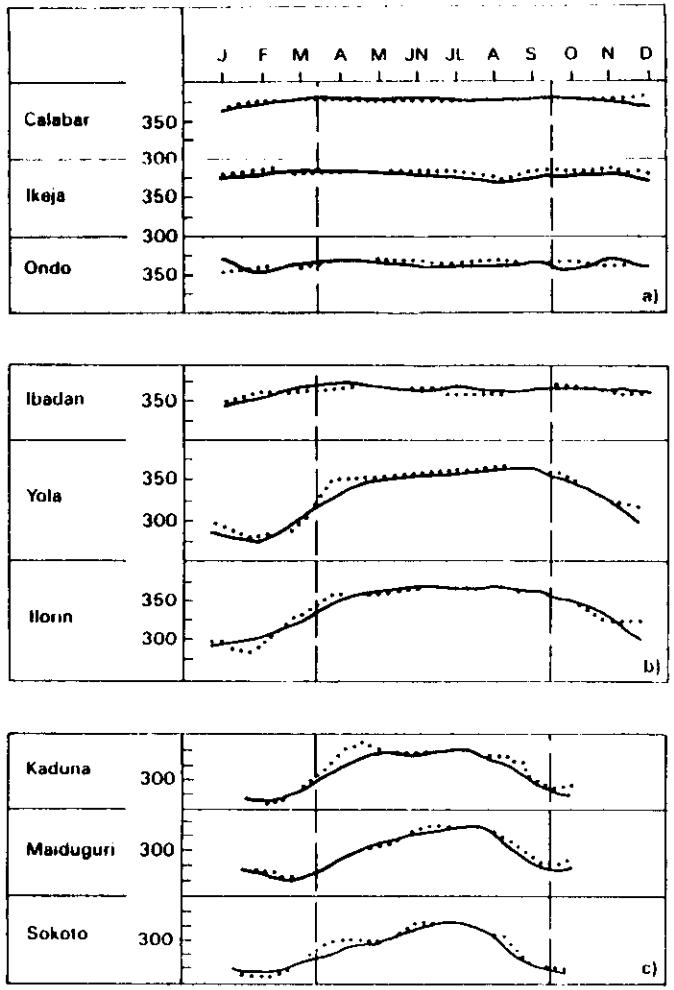

Figure 4 - Patterns of surface refractivity, N units in Nigeria for: a) southern zone, b) middle zone and c) northern zone (after Owolabi and Williams

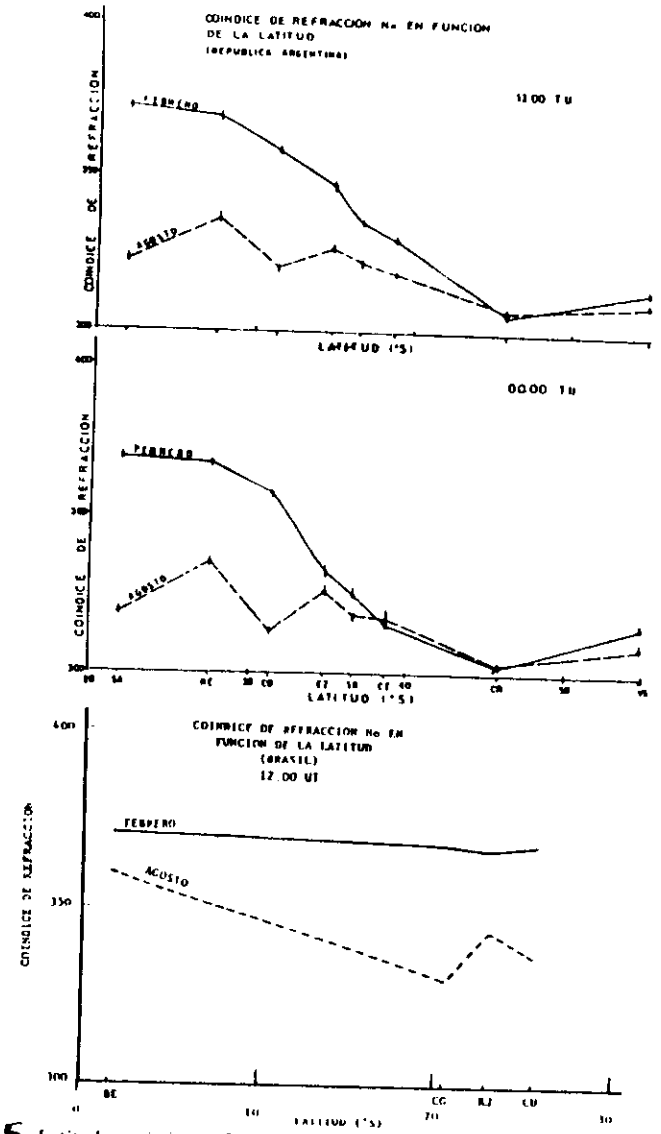

Fig. 5 Latitude variations of refractivity reduced to sea level in (a) Argentina and (b) Brazil.

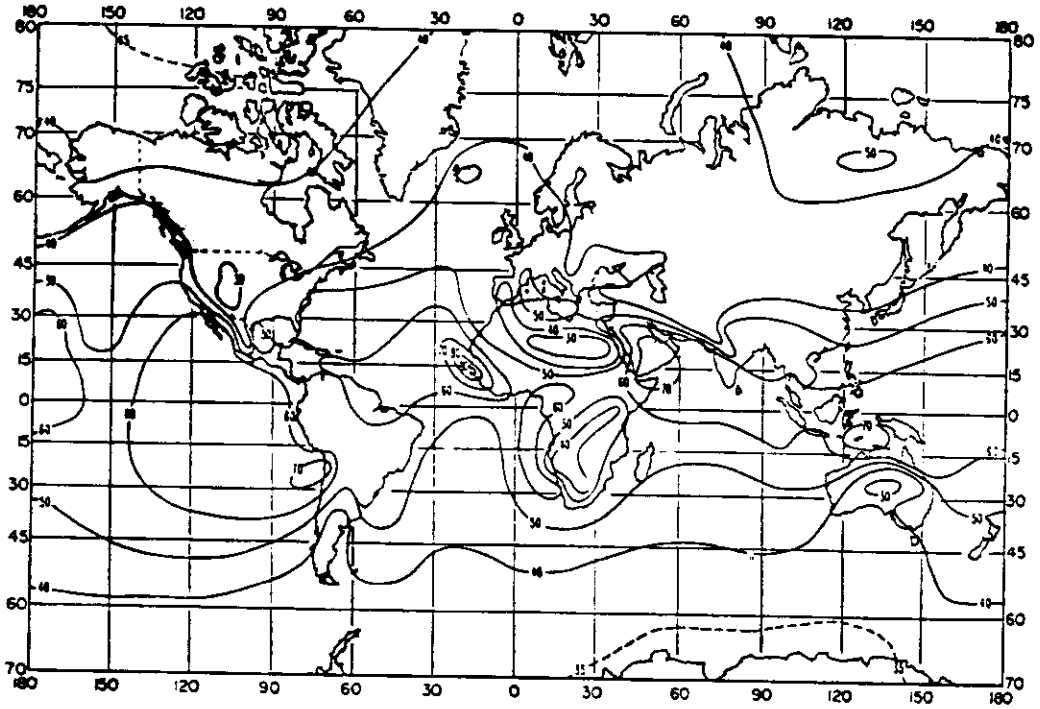

FIGURE 6 – *Monthly mean values of ΔV: November*

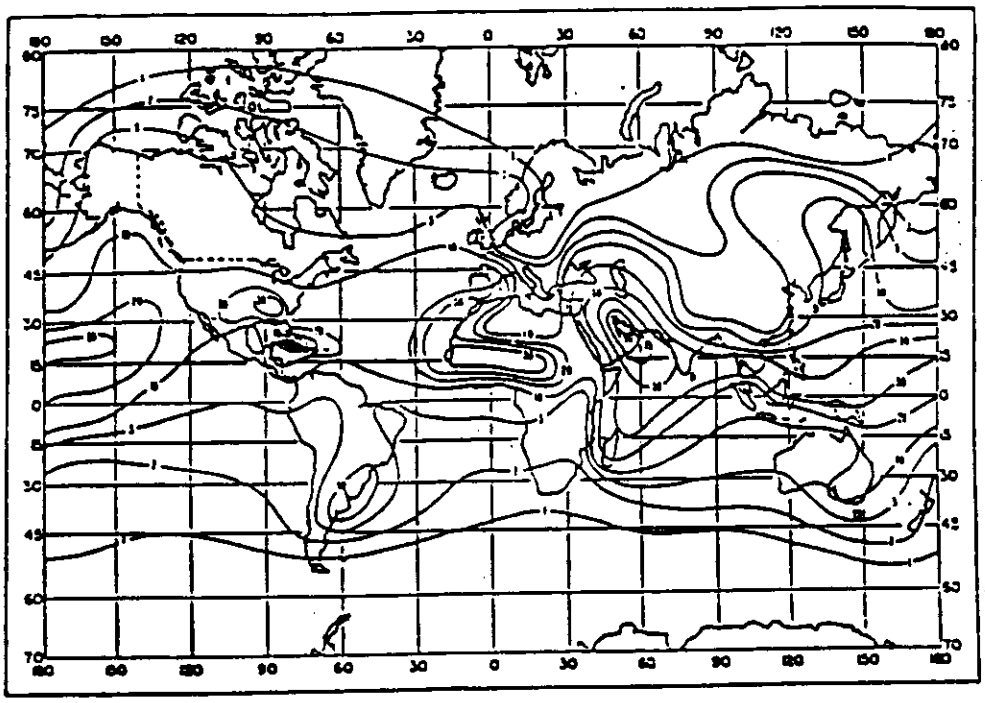

FIGURE 7 – *Percent of time gradient ≤ −100 (N/km): August*

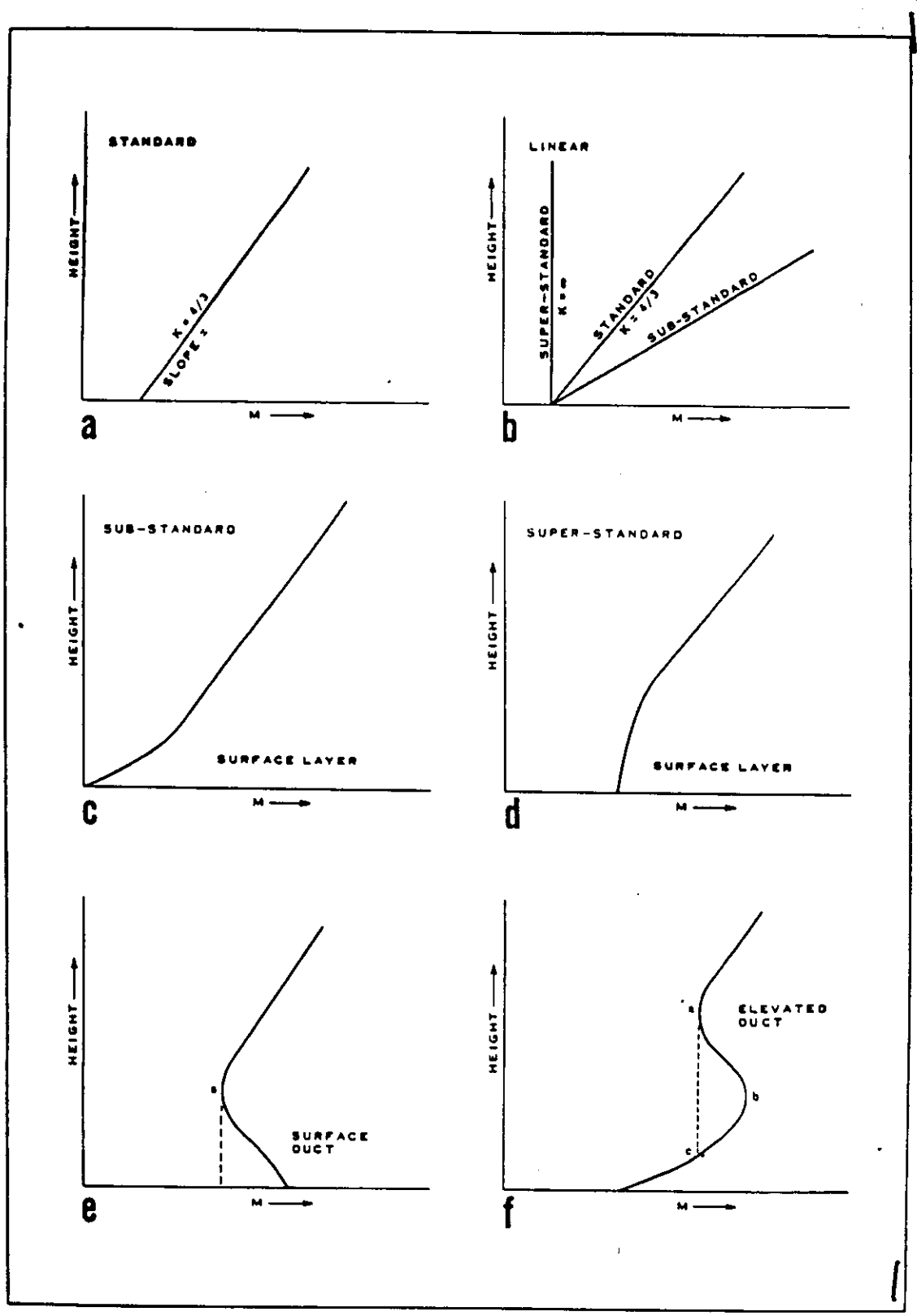

FIGURE 8
Typical M Profiles

[After Lenkurt, 1960]

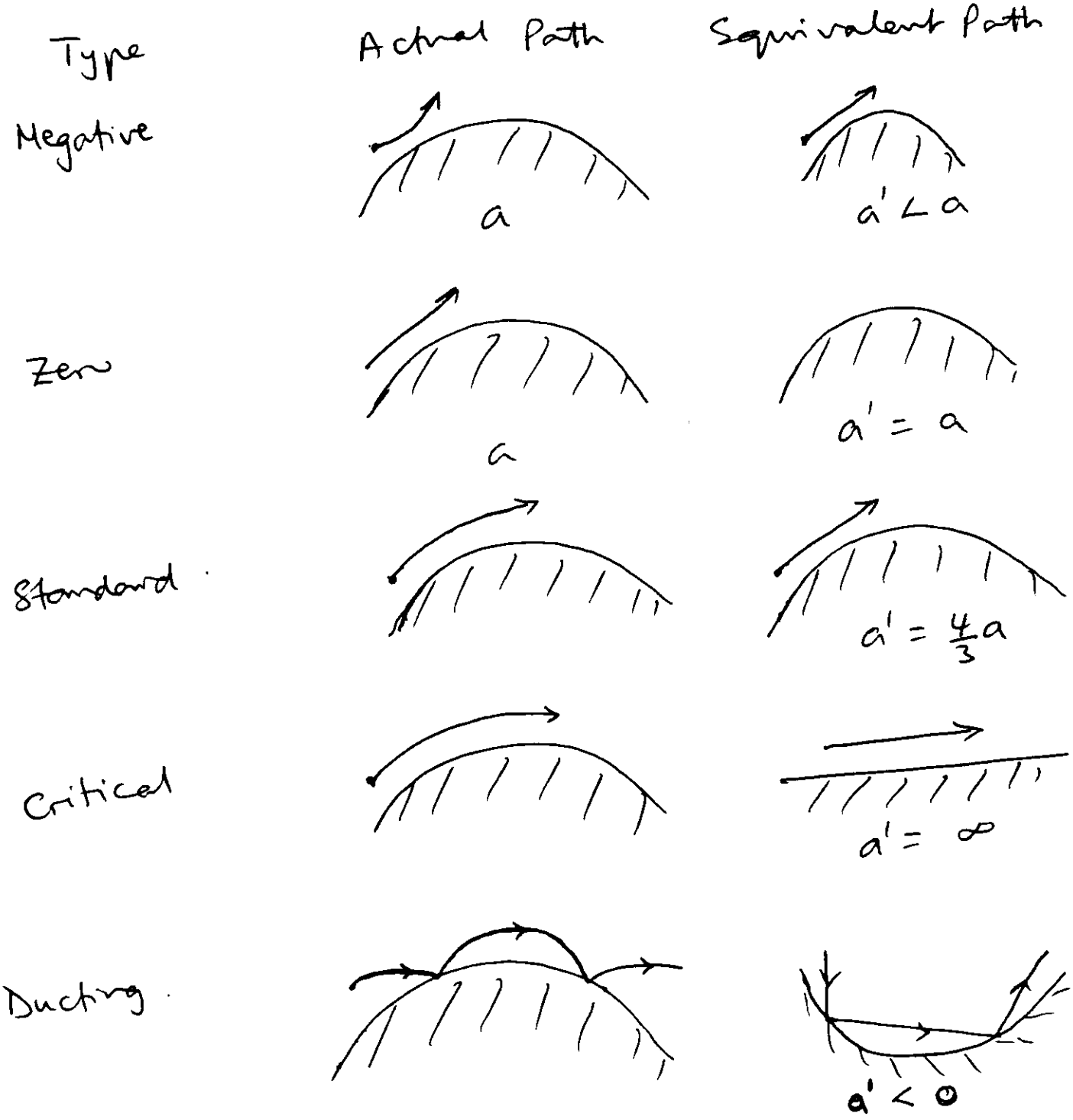

Fig 9 Actual and Equivalent paths.

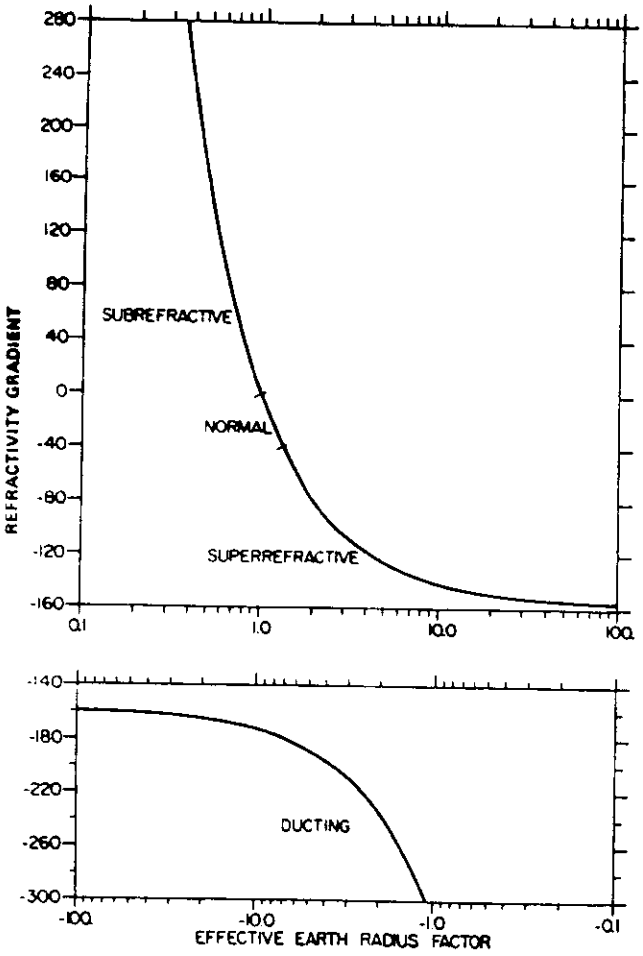

Figure 10: Effective earth radius factor as a function of refractivity gradient. dN/dh [Segal, 1977]

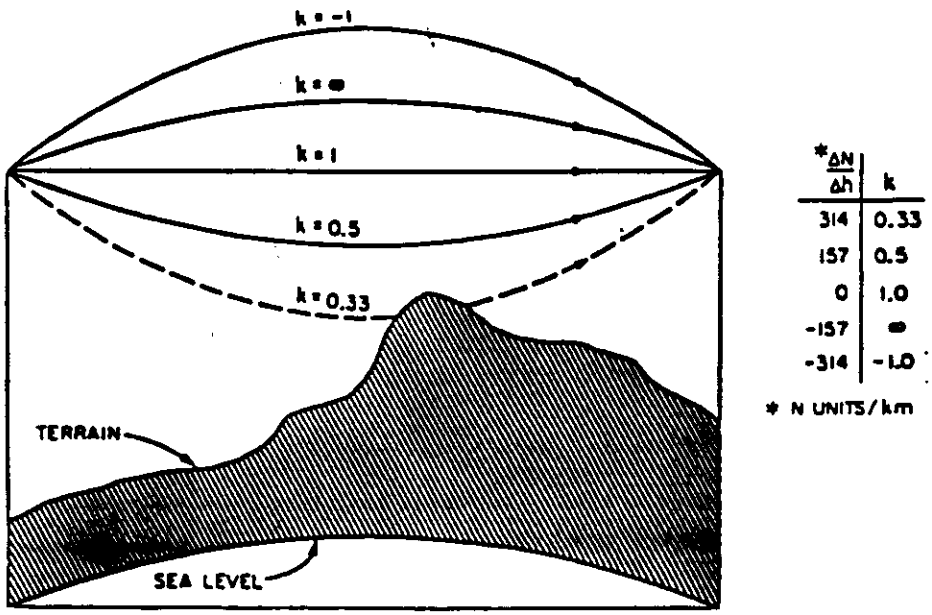

*ΔN/Δh	k
314	0.33
157	0.5
0	1.0
-157	∞
-314	-1.0

* N UNITS/km

FIGURE 11. THE BENDING OF RADIO RAYS FOR CONSTANT LINEAR REFRACTIVITY GRADIENTS from Dougherty

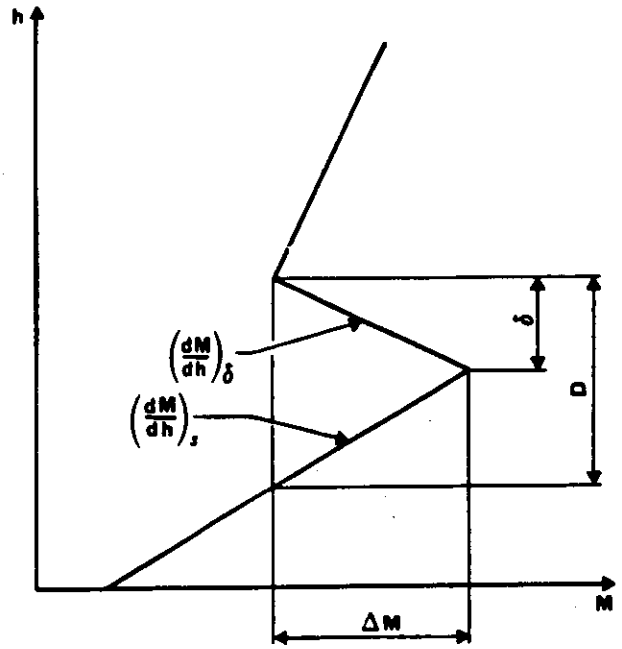

FIGURE 12 *Radiometric characteristics of a ducting layer* (CCIR, 1982)

δ: ducting layer thickness
D: tropospheric radio duct thickness

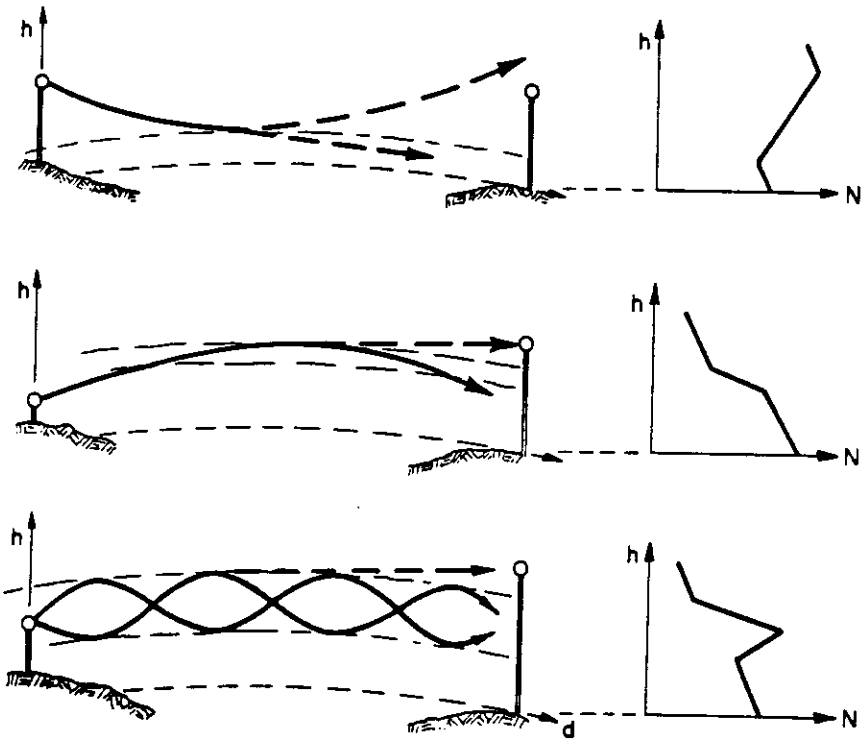

Figure 13 An atmospheric fading mechanism, Isolation. Isolation of terminals, one from another may be caused by atmospheric layers and ducts
[Dougherty & Dutton, 1981]

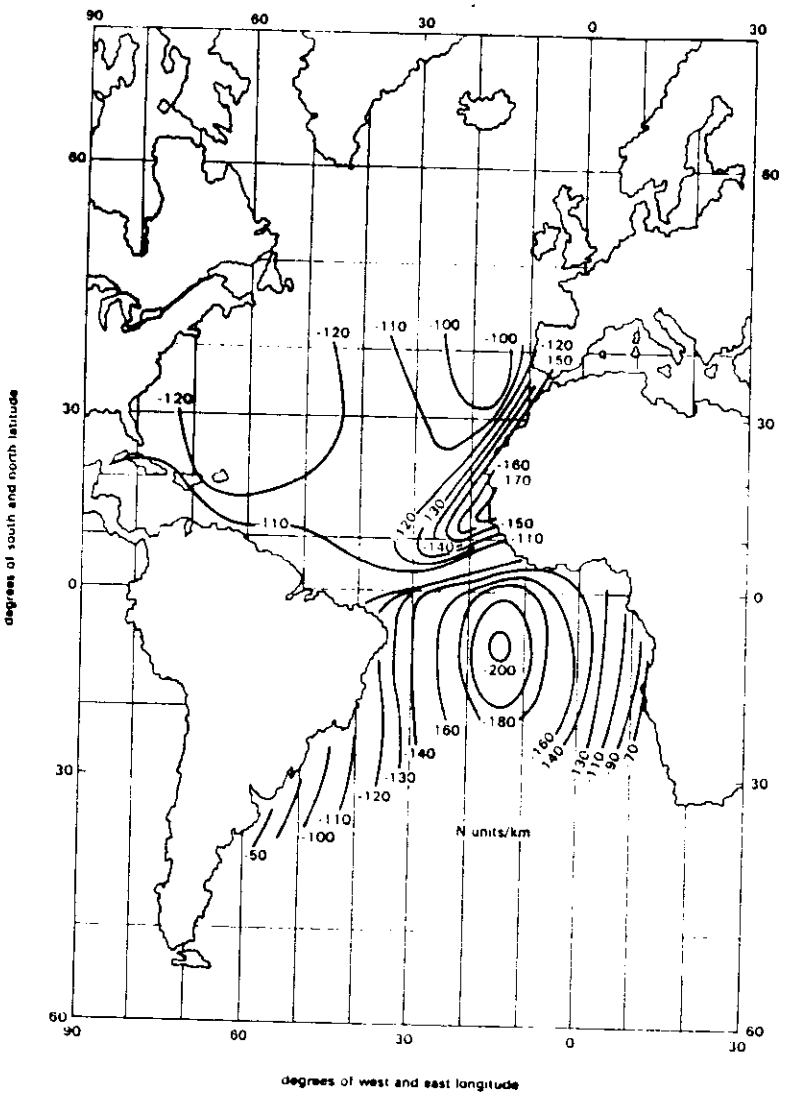

Fig. 14: Refractivity gradient contours for the trade wind inversion in May (after Dougherty et al. 1967)

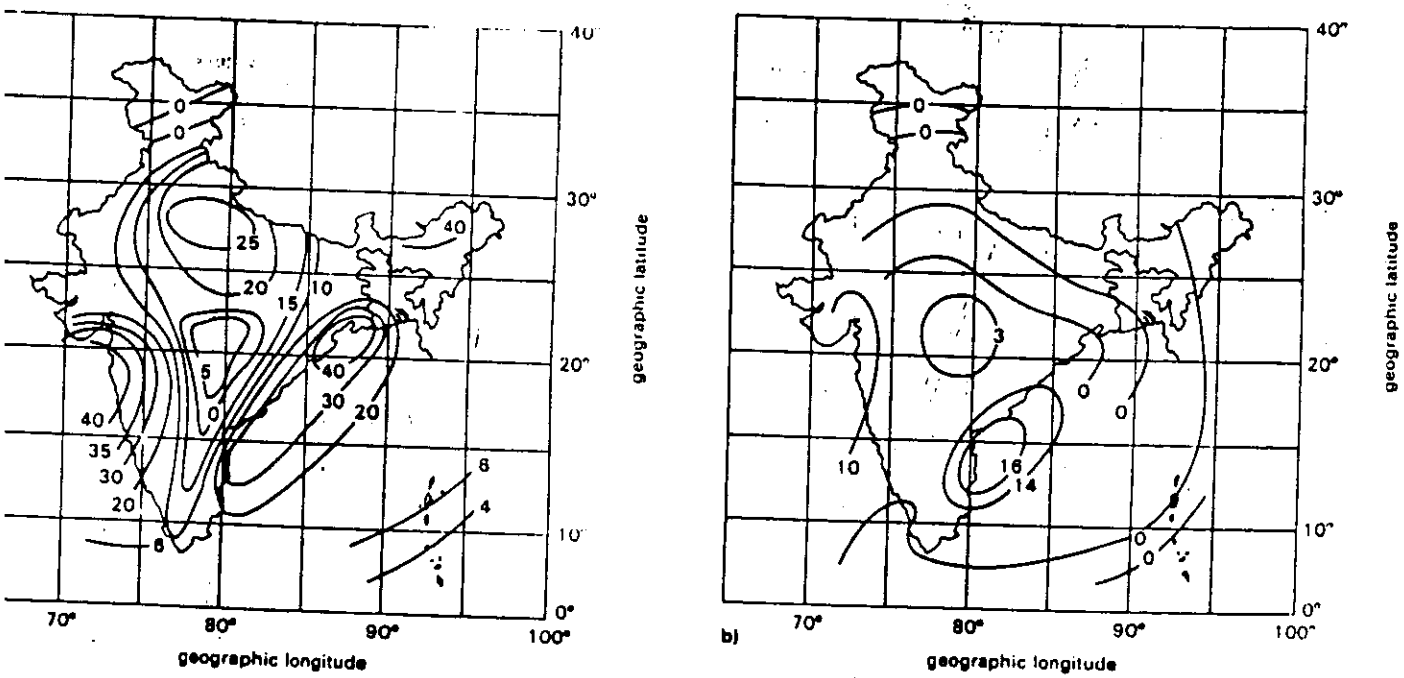

15: Surface duct occurrence probability (%) in India for (a) May and (b) July at 00h00 GMT [Reddy, 1982]

Fig. 16(a) SAAB fighter "Lansen" (A 32) with refractometer mounted under left wing.

[After Wickerts, 1976]

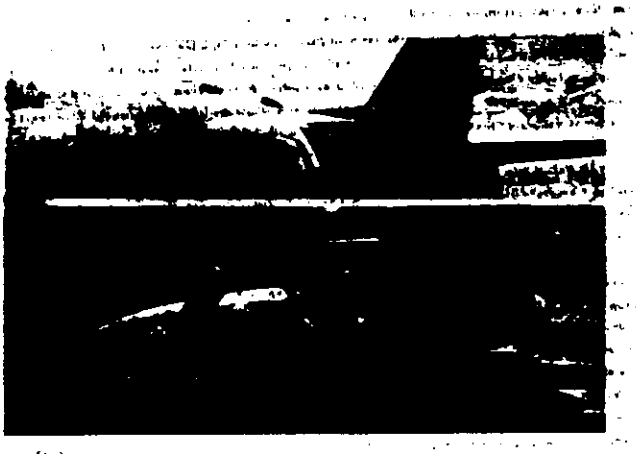

Fig. 16(b) The pod containing the instruments.

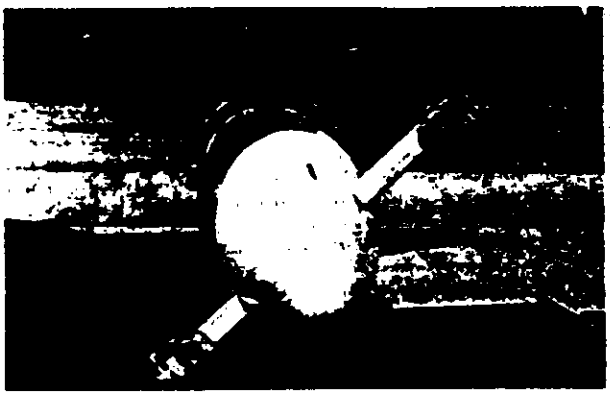

Fig 16c The two open cavities mounted on the pod.

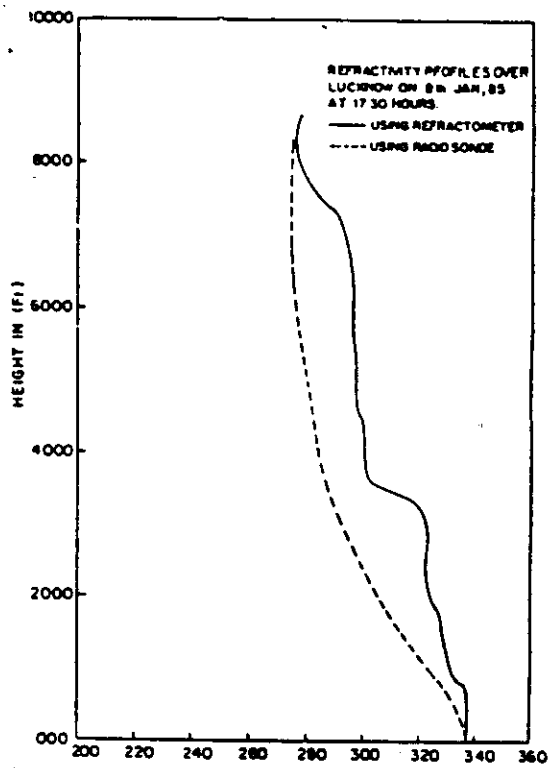

[After Reddy, 1987]

Fig. 17 *A comparison of refractivity profiles obtained from conventional Radio-Sonde and NPL Microwave Refractometer. Refractometer profiles were smoothed out for this comparison.*

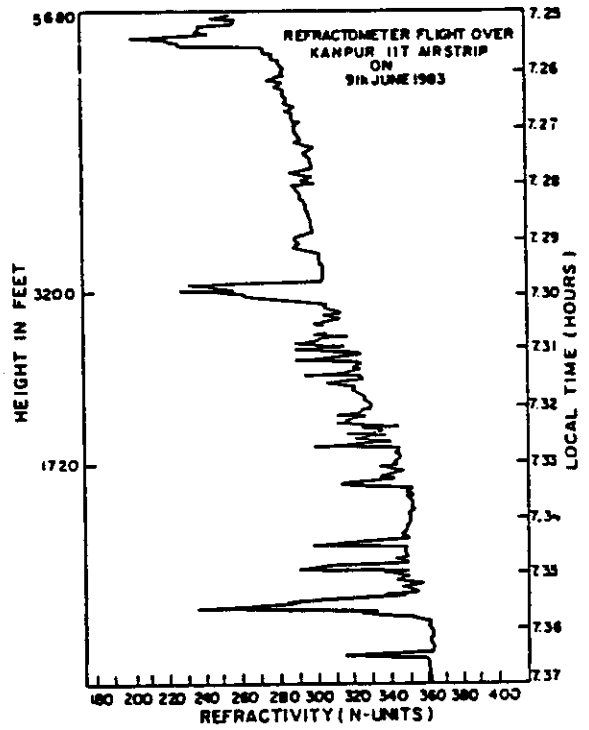

[After Reddy, 1987]

Fig. 18 *Actual refractivity profile showing the fine structure variation obtained by the NPL Microwave Refractometer aboard a CESSNA Aircraft over Kanpur.*

SOME METEOROLOGICAL CONDITIONS FAVORABLE FOR ANOMALOUS RADIO PROPAGATION

(a) Surface Superrefractive Layers ($\Delta N/\Delta h < -100$ N-units/km)

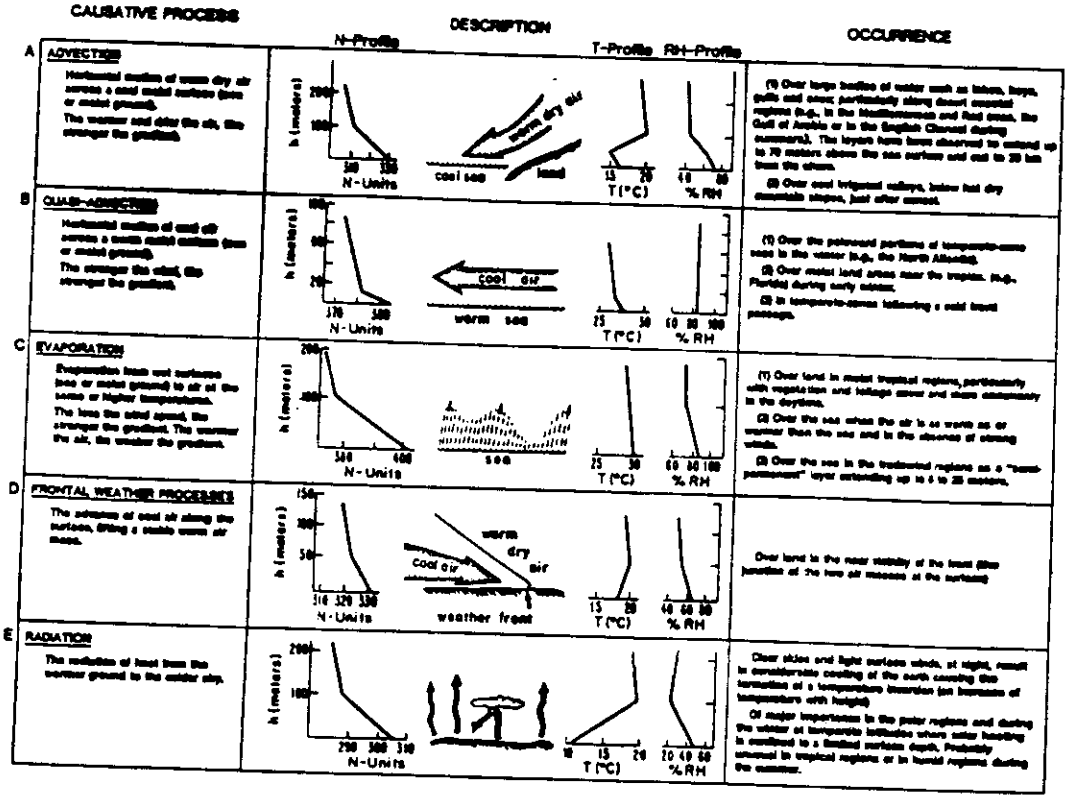

SOME METEOROLOGICAL CONDITIONS FAVORABLE FOR ANOMALOUS RADIO PROPAGATION

(b) Elevated Superfractive Layers ($\Delta N/\Delta h < -100$ N-Units/km)

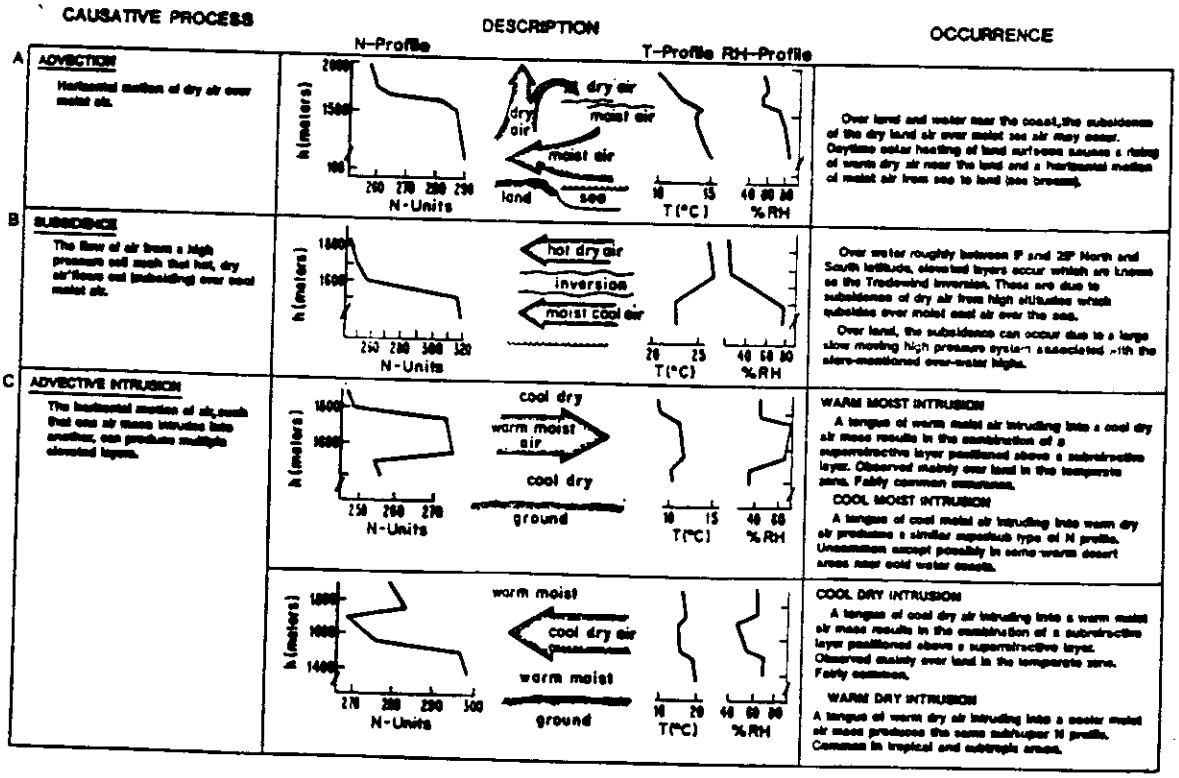

[After Dougherty and Dutton, 1981]